# Anomeric Dependence of Fluorodeoxyglucose Transport in Human Erythrocytes

Thomas M. O'Connell, Scott A. Gabel, and Robert E. London*

*Laboratory of Molecular Biophysics, National Institute of Environmental Health Sciences, Box 12233, Research Triangle Park, North Carolina 27709*

*Received February 15, 1994; Revised Manuscript Received July 12, 1994®*

ABSTRACT: The transport of several *n*-fluoro-*n*-deoxy-D-glucose derivatives across the human erythrocyte membrane has been studied under equilibrium exchange conditions using one- and two-dimensional nuclear magnetic resonance (NMR) techniques. This approach is based on the intracellular $^{19}F$ shift, which was found to depend on the anomeric form and on the F/OH substitution position. Since the transport behavior of both glucose anomers can be followed simultaneously, this approach is particularly sensitive to differences in anomeric permeability. For 2-, 3-, 4-, and 6-fluorodeoxyglucose analogs, the $\alpha$ anomers permeate more rapidly, and the $P_\alpha/P_\beta$ ratio is dependent on the position of fluorination, with values of 1.1, 1.3, 2.5, and 1.6, respectively, obtained at 37 °C. These results have been analyzed in terms of a simple alternating conformation model for the glucose transporter. Although mutarotase activity has been reported for red cells, mutarotation behavior for all anomers was found to be completely negligible on the transport and spin–lattice relaxation time scales. Metabolic transformation of the fluorinated glucose analogs, primarily to fluorinated gluconate and sorbitol analogs, is very slow and does not significantly interfere with the transport measurements. A mean ratio of 2.6 was found for the extracellular/intracellular fluorine spin–lattice relaxation rates.

The erythrocyte glucose transporter has served as a general model for transport by facilitated diffusion (Wheeler & Hinkle, 1985; Walmsley, 1988). Glucose is, however, a less than ideal subject for study as a consequence of the presence of two anomeric forms which may interact differently with the transporter, as well as the added complexity introduced by the possible presence of mutarotases (Sachs, 1968). As discussed, for example, by Gorga and Lienhard (1981), differences in the velocity constants ($V_m$) or affinities ($K_m$) of the transporter for the two glucose anomers can have a significant influence on the interpretation of transport data in terms of various proposed models for the transporter. Indeed, it would not be surprising for this to be the case since a change in configuration of other hydroxyl groups, e.g., in going from glucose to galactose, has a major (>10-fold) effect on the measured transport parameters (Barnett et al., 1973). This situation is further complicated by the difficulties of measuring high rates of transport, which characterize the glucose transport system at physiological temperatures. As discussed by Alger and Prestegard (1979), unstirred layer diffusion can rate-limit the observed flux, requiring the use of specialized apparatus to obtain useful data. Alternatively, NMR[1] methods which utilize magnetization transfer to study equilibrium exchange processes become more useful at higher temperatures, as transport rates become more competitive with spin–lattice relaxation rates. Such studies also provide a natural solution to the anomer selectivity problem, since resonances from each anomeric form are frequently resolvable.

The intracellular $^{19}F$ shift which allows the resolution of resonances corresponding to intra- and extracellular compounds (London & Gabel, 1989) can be exploited for determination of transport behavior of fluorinated compounds. This approach has recently been utilized in studies of the transport of 3FDG by erythrocytes (Potts et al., 1990; Potts & Kuchel, 1992). In such applications, the fluorine nucleus serves the multiple purposes of allowing observation of intra- and extracellular FDG pools as well as retarding the metabolism of the fluorinated compounds so that relatively long-term NMR studies can be carried out. However, the substitution of the fluorine nucleus for a hydroxyl group also alters the interaction of the glucose with both solvent and transporter, and this can serve to test various hypotheses regarding the glucose–transporter interaction (Barnett et al., 1973; Riley & Taylor, 1973; Lopes & Taylor, 1979). In addition to questions regarding transport mechanism, characterization of the transport behavior of fluorinated glucose analogs is important in view of their use in PET scanning (Tewson et al., 1978; Vyska et al., 1985).

## MATERIALS AND METHODS

2-Fluoro-2-deoxy-D-glucose and 3-fluoro-3-deoxy-D-glucose were obtained from Omicron Biochemicals, Inc. (South Bend, IN), and 4-fluoro-4-deoxy-D-glucose and 6-fluoro-6-deoxy-D-glucose were obtained from Sigma (St. Louis, MO). One- and two-dimensional proton-decoupled fluorine NMR experiments were carried out at 470.5 MHz on a GE GN-500 NMR spectrometer using a 5-mm $^{19}F\{^1H\}$ probe. Field homogeneity was optimized by shimming on the $H_2O$ resonance, with a typical line width <0.05 ppm. Blood samples were prepared using donated human blood obtained from the American Red Cross. The blood was platelet-free, and the plasma and buffy coat were discarded after centrifugation. The cells were then washed three times in 5 volumes of saline buffer solution containing 123 mM NaCl, 15 mM Tris–HEPES (pH 7.4), 5 mM ascorbic acid, and 10 mM fluorinated sugar. In several of the studies, a somewhat higher osmolarity buffer, in which 40 mM phosphate replaced the 15 mM Tris-HEPES, was used. The higher osmolarity increases the chemical shift difference between intra- and extracellular resonances and was particularly useful for the studies involving 2-fluoro-2-deoxyglucose, for which the resonances of the intracellular $\alpha$-FDG and extracellular $\beta$-FDG are not baseline resolved. A

® Abstract published in *Advance ACS Abstracts,* August 15, 1994.

[1] Abbreviations: FDG, fluorodeoxy-D-glucose; nFDG, *n*-fluoro-*n*-deoxy-D-glucose, where *n* = 2, 3, 4, or 6; NMR, nuclear magnetic resonance; EXSY, exchange spectroscopy; PET, positron emission tomography.

stream of carbon monoxide was passed over the cells for approximately 30 s with gentle stirring in order to remove any paramagnetic deoxyhemoglobin, which can broaden the resonances. Samples were not spun in order to prevent centrifugation effects on the cells. The hematocrits of the samples were measured using capillary tubes spun on a microhematocrit centrifuge.

The two-dimensional exchange spectroscopy (EXSY) experiment is based on the original 2D EXSY sequence of Macura and Ernst (1980). The sequence is as follows:

$$^{19}\text{F:}\quad (\pi/2)_x - t_{1/2} - t_{1/2} - (\pi/2)_{x/y} - t_{\text{mix}} - (\pi/2)_x \quad \text{acquire}$$

$$^{1}\text{H:}\qquad\qquad -\pi- \qquad\qquad \text{decouple}$$

Proton decoupling is provided in the directly detected dimension using the $^1$H decoupler during acquisition and in the second dimension using the $^1$H $\pi$ refocusing pulse in the middle of the $t_1$ evolution period. The data were acquired in hypercomplex mode with alternate scans stored in separate blocks. The $^{19}$F $\pi/2$ pulse length was calibrated at 23 $\mu$s and the $^1$H $\pi$ pulse length was 150 $\mu$s. The spectral widths of the two-dimensional experiments were 1600, 3600, and 2000 Hz for the 2-fluoro-, 3-fluoro-, and 4-fluorodeoxyglucose isomers, respectively. Each spectrum was digitized using 2048 points in the directly detected dimension and 64 points in the second dimension which was later zero-filled to 512 points. An interpulse delay of 8 s was used, which was longer than $5T_1$. The 2D data were processed using the GE GEM software. Exponential multiplication was used in processing all of the spectra. The peak resolution obtainable with each of the isomers dictated the use of different degrees of apodization.

One-dimensional magnetization transfer studies were carried out using the selective inversion technique of Robinson et al. (1985), which has the advantage that frequency selective pulses are not required. The analysis of the data was based on the approach described by Perrin and Engler (1990) in which two series of experiments are carried out with the resonance of the intracellular glucose species or the extracellular glucose selectively inverted using the sequence

$$\pi/2_x - t_1 - \pi/2_x - t_2 - \pi/2_\phi \quad \text{acquire}$$

where $t_1 = 1/(2|\nu_i - \nu_e|)$, $t_2$ is the variable delay during which transfer of magnetization occurs, and the carrier frequency of the radiofrequency is set at the position of the resonance which is selectively inverted. The phase $\phi$ of the final $\pi/2$ pulse and the receiver are cycled through $x, y, -x, -y$.

The data for the one- and two-dimensional studies were then analyzed by matrix diagonalization methods to obtain the elements of the relaxation matrix **R**, in which the diagonal elements correspond to $1/T_{1o} + k_{oi}$ and $1/T_{1i} + k_{io}$ and the off-diagonal elements correspond to $k_{oi}$ and $k_{io}$. Here $k_{io}$ and $k_{oi}$ are the apparent first-order rate constants for efflux and influx, respectively, and $T_{1o}$ and $T_{1i}$ are the spin–lattice relaxation times for the extracellular and intracellular species, respectively. Although, in principle, both experiments can be analyzed using a 4 × 4 matrix which connects intra- and extracellular $\alpha$ and $\beta$ resonances, it was found that there was no cross peak or cross relaxation between $\alpha$ and $\beta$ resonances of either the intra- or extracellular FDG pools on the spin–lattice relaxation time scale. Hence, the data for the $\alpha$ and $\beta$ resonances were analyzed separately using 2 × 2 matrices. Briefly, the one-dimensional data are organized into a series of 2 × 2 matrices, $\mathbf{M}(t_m)$, corresponding to each time point, and analyzed by matrix methods (Perrin & Engler, 1990) according to the relation

Table 1: Intracellular Shifts at Neutral pH[a]

| molecule | $\beta_i - \beta_e$ (ppm) | $\alpha_i - \alpha_e$ (ppm) | $\Delta\beta - \Delta\alpha$ (Hz) |
|---|---|---|---|
| | at 10 mM concentration | | |
| 2FDG | 0.245 | 0.217 | 18.8 |
| 3FDG | 0.239 | 0.222 | 8.0 |
| 4FDG | 0.200 | 0.209 | −4.2 |
| 6FDG | 0.239 | 0.261 | −10.3 |
| | at 0.2 mM concentration | | |
| 2FDG | 0.269 | 0.239 | 14.1 |
| 3FDG | 0.262 | 0.244 | 8.5 |
| 4FDG | 0.230 | 0.231 | −5.2 |
| 6FDG | 0.260 | 0.282 | −10.3 |

[a] Spectra obtained at 37 °C and a spectral resolution of 0.9 Hz (0.002 ppm)

$$\ln\left[(\mathbf{M} - \mathbf{M}_{eq})\cdot(\mathbf{M}_o - \mathbf{M}_{eq})^{-1}\right] = X(\ln \Lambda)X^{-1} = -t_m\mathbf{R} \quad (1)$$

where $\mathbf{M}_o$ corresponds to the data matrix at $t_m = 0$, $\mathbf{M}_{eq}$ is the matrix of the fully relaxed system, and $X$ is a square matrix of eigenvectors that transforms $(\mathbf{M} - \mathbf{M}_{eq})\cdot(\mathbf{M}_o - \mathbf{M}_{eq})^{-1}$ into the diagonal matrix $\Lambda$. A linear fit of the data then yields the relaxation matrix. For the two-dimensional experiment, $\mathbf{M} - \mathbf{M}_{eq}$ is obtained directly by integration of the peak volumes in the 2D spectrum, and the data can be fitted linearly. Reproducibility of the measurements on the same samples is very high; repeated measurements on the same sample give variations which are always under 5% and generally under 2%. Alternatively, sample-to-sample variations are larger, reflecting both the inherent biological variability as well as the fact the various experimental parameters, concentrations, pH values, sample temperature, etc., although nominally the same, are not identical. Standard deviations of the rate constants stated in Table 2 correspond to measurements on at least five samples for each of the fluorodeoxyglucose isomers studied.

## RESULTS

*Chemical Shifts and Metabolism.* The $^{19}$F NMR spectra of 2-, 3-, 4-, and 6-fluorodeoxyglucose show separate resonances corresponding to intra- and extracellular glucose pools. As is the case with most properties of sugars, the chemical shift difference between the two pools was found to exhibit an anomeric dependence, with a larger shift for the $\beta$ anomers of 2-FDG and 3-FDG, a larger shift for the $\alpha$ anomer of 6-FDG, and a $\Delta\beta - \Delta\alpha$ shift difference near zero for 4-FDG. The difference between the shifts of the two anomers as a function of the position of fluorine substitution is shown in Table 1. Although the basis for the intracellular shift is not yet unambiguously established, it appears that, as in the case of phosphorus-containing molecules, the chemical shift difference is related to differences in the extent of hydrogen bonding between the intra- and extracellular pools (Kirk & Kuchel, 1988; Xu et al., 1993). Analogous to $^{31}$P NMR studies of dimethyl methylphosphonate (DMMP) in erythrocyte suspensions (Kirk & Kuchel, 1985), increasing the ionic strength of the buffer by increasing the NaCl concentration led to further increases in $\delta_{\text{intracellular}} - \delta_{\text{extracellular}}$. This is a consequence of the reduction in cellular volume, which effectively increases the intracellular protein concentration. The increase in shift with pH for both the $\alpha$ and $\beta$ anomers of 3FDG showed a slight curvature, analogous to the DMMP study. Using an approximate linear fit, we obtain slopes of $1.3 \times 10^{-3}$ and $1.1 \times 10^{-3}$ ppm/mM for the $\beta$ and $\alpha$ anomers, respectively. Increasing [NaCl] from 123 to 323 mM doubled the magnitude of $\delta_{\text{intra}} - \delta_{\text{extra}}$ and, in light of the difference in slope noted above for the two anomers, also increased the $\Delta\beta - \Delta\alpha$ shift difference.

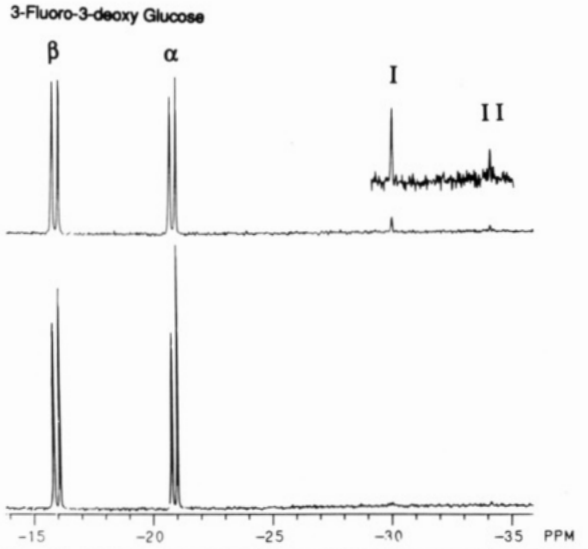


FIGURE 1: Proton-decoupled $^{19}F$ spectra of 3-fluoro-3-deoxyglucose in a suspension of erythrocytes ($H_t = 0.6$) immediately after addition of 10 mM 3FDG (lower trace) and after an 18-h incubation period at room temperature (upper trace). For each anomer, the downfield (upfield) resonance corresponds to the intracellular (extracellular) glucose. Metabolites I and II are assigned to 3-fluoro-3-deoxygluconate and/or the 6-phosphogluconate and to 3-fluoro-3-deoxysorbitol, respectively.

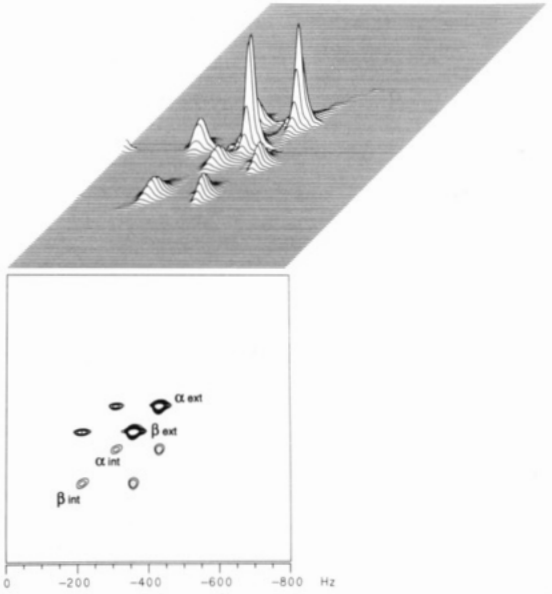


FIGURE 2: Two-dimensional EXSY contour (lower) and stacked plots (upper) of 2-fluoro-2-deoxyglucose in the presence of human erythrocytes. The spectra correspond to a mixing time of 400 ms. The diagonal resonances corresponding to intra- and extracellular $\alpha$- and $\beta$-D-glucose resonances are labeled, and the cross-peak intensities are proportional to the rates of interconversion. As is apparent from these figures, interconversion of the $\alpha$ and $\beta$ anomers is insignificant on the exchange time scale.

Fluorinated sugars are known to be metabolized in a variety of cell types (Nakada & Kwee, 1986; Nakada et al., 1986; Kanazawa et al., 1987; Kojima et al., 1988; Berkowitz et al., 1990; Karino et al., 1991), but our observation of the 2-, 3-, and 4-fluorodeoxyglucose in erythrocytes indicate that such metabolic processes are slow. A $^{19}F$ NMR spectrum of an erythrocyte suspension observed 18 h after the addition of 3FDG is shown in Figure 1. In addition to the intra- and extracellular glucose resonances, resonances corresponding to 3-fluoro-3-deoxygluconate and/ or its 6-phosphate ester (metabolite I) and to 3-fluorosorbitol (metabolite II) are readily observed. The latter metabolite similarly exhibits two resonances, corresponding to intra- and extracellular 3-fluorosorbitol; however, the gluconate resonances are not similarly doubled, indicating that the charged metabolite remains intracellular. This observation is consistent with the conclusion that metabolite I corresponds to 3-fluoro-3-deoxygluconate 6-phosphate. At lower 2FDG concentrations, the $^{19}F$ spectra of 2-fluorodeoxyglucose showed additional resonances 3 ppm downfield of the free $\beta$-2FDG glucose, which can similarly be assigned to 2-fluoro-2-deoxygluconate and/or its 6-phosphate derivative (Nakada & Kwee, 1986). In all cases, metabolic transformations were sufficiently slow not to interfere significantly with transport studies using magnetization transfer techniques.

*Transport Rate Determination.* As a consequence of the possible significance of mutarotation and the possible presence of mutarotase activity, it is necessary to consider the exchange problem as potentially a four-site process, involving intra- and extracellular $\alpha$ and $\beta$ fluorodeoxyglucose resonances. For this reason, the problem was initially approached using the two-dimensional EXSY experiment (Macura & Ernst, 1980). A typical plot for 2-fluoro-2-deoxygluocse obtained using a 400-ms mixing time is shown in Figure 2. The one-dimensional spectrum shows four resonances corresponding to the intra- and extracellular $\alpha$- and $\beta$-FDG pools. As is apparent from this figure, no cross peaks are observable corresponding to the $\alpha$–$\beta$ transition, indicating that such processes are completely negligible at this mixing time. In contrast, pronounced cross peaks are readily observed connecting intra- and extracellular 2FDG resonances. Hence, the equilibrium exchange rate of 2FDG is readily obtained using this technique. The exchange behavior observed in these studies arises due to the activity of the erythrocyte glucose transporter. Addition of the transport inhibitor cytochalasin B (0.2 mM) (Krupka & Deves, 1980) completely eliminates the cross peaks.

Similar EXSY spectra obtained for the $\alpha$ and $\beta$ resonances of 3-fluoro-3-deoxyglucose and 4-fluoro-4-deoxyglucose derivatives are shown in Figures 3 and 4. In these cases, the $\alpha$ and $\beta$ resonance shift differences are much larger relative to the intracellular shift, so that we have plotted each region of the spectra separately. However, analogous to the case of 2FDG shown above, no cross peaks connecting $\alpha$ and $\beta$ resonances of 3FDG or 4FDG were observed, indicating that such processes are negligible on this time scale. One of the unexpected results of these studies is the observation that the apparent anomeric dependence of the transport rate depends significantly on the site of fluorine substitution. Thus, as is apparent from observations of the stacked plots shown in Figures 2, 3 and 4, the $\alpha$ and $\beta$ anomers of the 2-fluoro-2-deoxyglucose and 3-fluoro-3-deoxyglucose are transported at fairly similar rates, with the permeability ratio $P_\alpha/P_\beta$ typically slightly greater than 1. Alternatively, for the 4-fluoro-4-deoxyglucose, there is a very significant difference in the rate, with $P_\alpha/P_\beta$ ratios $\sim$2.5, as discussed below. The 6-fluoro derivative exhibited an intermediate ratio of 1.6.

Transport rates and the corresponding permeabilities were determined either by analysis of the two-dimensional EXSY data obtained for a series of mixing times, typically 0.2, 0.4, 0.6, and 0.8 s, or by one-dimensional inversion transfer methods (Perrin & Engler, 1990). The latter approach is more easily implemented for a two-state system. Since, as shown above, the $\alpha \leftrightarrow \beta$ interconversion rates are apparently negligible on the transport time scale, the $\alpha$ and $\beta$ transport can be determined in separate studies. The 1D approach offers the advantage that data for a series of delays can be obtained on the sample in a relatively short period of time. The particular approach used for the present studies involves combining the data from two series of studies in which either the intra- or

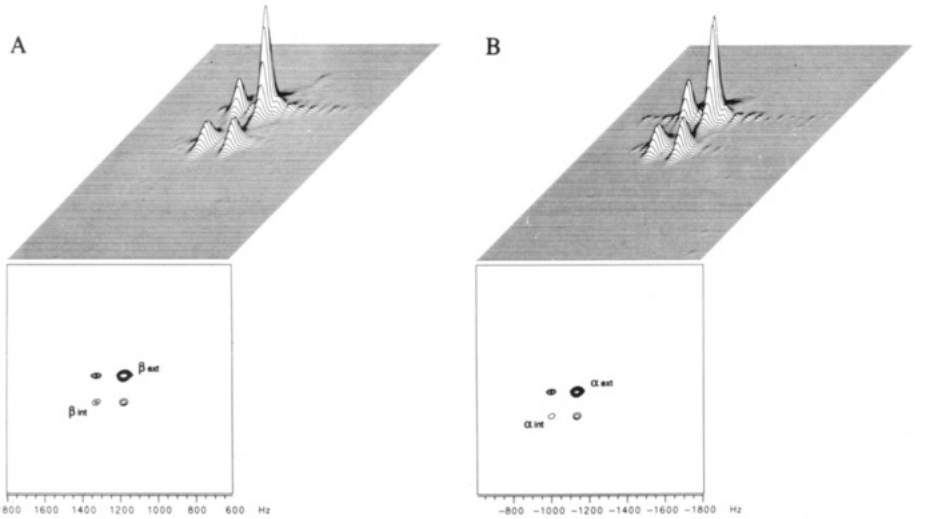


FIGURE 3: Two-dimensional EXSY contour (lower) and stacked plots (upper) of 3-fluoro-3-deoxyglucose in the presence of human erythrocytes. Since no cross-peak intensity was observed connecting the $\alpha$ and $\beta$ anomers, only the regions containing the $\beta$ (A) and $\alpha$ (B) resonances are shown. The spectra correspond to a mixing time of 400 ms.

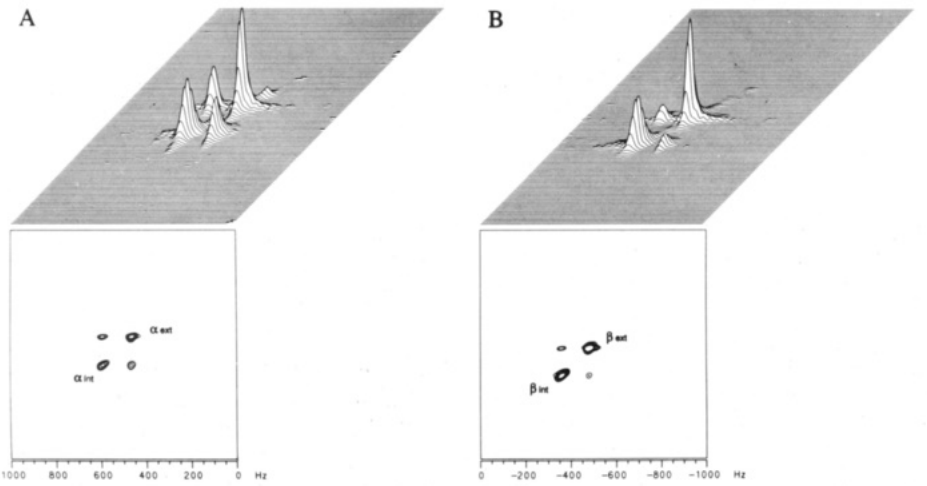


FIGURE 4: Two-dimensional EXSY contour (lower) and stacked plots (upper) of 4-fluoro-4-deoxyglucose in the presence of human erythrocytes. As in the case of the 3-fluoro compound, no cross-peak intensity was observed connecting the $\alpha$ and $\beta$ anomers, and only the regions containing the $\alpha$ (A) and $\beta$ (B) resonances are shown. The spectra correspond to a mixing time of 400 ms. The anomeric dependence of the transport rate is clearly evident from a comparison of the figures.

extracellular resonance is initially inverted, and measurements are made after varying delays. The analysis of the equilibrium exchange data using the 1D inversion transfer method is illustrated for the case of 6FDG in Figure 5, which shows the time dependence of two of the four elements of the relaxation matrix: $R_{11} = 1/T_{1i} + k_{-1}$ and $R_{21} = -k_{-1}$. As discussed in Materials and Methods, the matrix diagonalization converts the time-dependent magnetizations which are sums of exponentials into a linear relation for the elements of the relaxation matrix as a function of the delay $t_2$. Data in Figure 5 correspond to the $\alpha$ and $\beta$ fluorine resonances of 6-FDG, and the significant dependence of $k_{-1}$ on the anomeric configuration is readily apparent. Mean values of the corresponding efflux rate constants, $k_{-1}$, and intra- and extracellular spin–lattice relaxation rates obtained from the 1D and 2D studies are summarized in Table 2. Permeabilities, calculated as described below, and fractional concentrations $f_i$ of each anomeric form are also given. As noted above, $P_\alpha/P_\beta$ ratios for the fluorinated glucose derivatives are slightly greater than 1 for fluorine substitution at positions 2 or 3, but larger for substitution at positions 4 or 6.

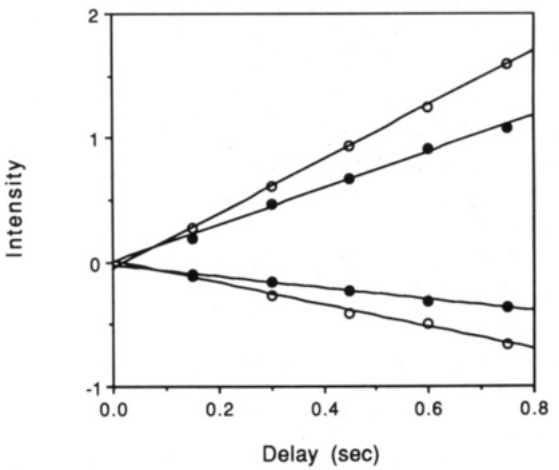


FIGURE 5: Time dependence of two of the four relaxation matrix elements: $R_{11} = 1/T_{1i} + k_{-1}$ (having positive slope) and $R_{21} = -k_{-1}$ (having negative slope), where $k_{-1}$ is the efflux rate constant. The open and closed symbols correspond to $\alpha$- and $\beta$-6FDG, respectively.

At equilibrium, the influx and efflux rate constants are related to the ratio of the intracellular/extracellular glucose concentrations. If the glucose is not significantly metabolized and is distributed according to the available intra- and extracellular volumes, $V_i$ and $V_e$, this condition can be written as

Table 2: Measured Efflux Rate Constants, Relaxation Rate Constants, and Calculated Permeabilities

| molecule | $k_{-1}$[a] ($s^{-1}$) | permeability (cm $s^{-1}$) | $R_{1i}$ ($s^{-1}$) | $R_{1o}$ ($s^{-1}$) | $f_i$[b] |
|---|---|---|---|---|---|
| α-2FDG | 1.29 ± 0.31 | 5.48 ± 1.32 × $10^{-5}$ | 1.03 ± 0.28 | 0.31 ± 0.11 | 0.44 |
| β-2FDG | 1.21 ± 0.22 | 5.15 ± 0.94 × $10^{-5}$ | 1.15 ± 0.20 | 0.42 ± 0.06 | 0.56 |
| α-3FDG | 1.35 ± 0.32 | 5.77 ± 1.37 × $10^{-5}$ | 1.19 ± 0.08 | 0.50 ± 0.04 | 0.48 |
| β-3FDG | 1.04 ± 0.23 | 4.44 ± 0.98 × $10^{-5}$ | 1.10 ± 0.16 | 0.56 ± 0.04 | 0.52 |
| α-4FDG | 0.77 ± 0.16 | 3.27 ± 0.69 × $10^{-5}$ | 0.95 ± 0.04 | 0.36 ± 0.04 | 0.41 |
| β-4FDG | 0.30 ± 0.09 | 1.29 ± 0.39 × $10^{-5}$ | 0.99 ± 0.04 | 0.38 ± 0.08 | 0.59 |
| α-6FDG | 0.72 ± 0.21 | 3.07 ± 0.81 × $10^{-5}$ | 1.19 ± 0.09 | 0.33 ± 0.08 | 0.40 |
| β-6FDG | 0.44 ± 0.20 | 1.87 ± 0.60 × $10^{-5}$ | 1.07 ± 0.11 | 0.52 ± 0.10 | 0.60 |

[a] Errors are standard deviations, $n = 5$. Results of one- and two-dimensional NMR studies were averaged together. [b] $f_i$ is the fractional concentration of the corresponding anomer.

$$k_1 V_e = k_{-1} V_i \tag{2}$$

The inward permeability, $P_1$, is related to the inward rate constant determined from the NMR measurements by the relation

$$P_1 = \frac{V_e}{A} k_1 = \frac{\mathrm{MCV}(1 - H_t)}{A_{cell}(H_t)} k_1 \tag{3}$$

where $H_t$ is the hematocrit, $V_e$ is the extracellular volume/mL equal to $V_o(1 - H_t)$, $A_{cell} = 1.43 \times 10^{-6}$ cm$^2$ is the surface area/cell, $A$ is the total surface area, equal to $(A_{cell}H_t)/\mathrm{MCV}$, and MCV is the mean cell volume, equal to 85 fL for red cells in isotonic solution (Chapman & Kuchel, 1990). Similarly, the outward permeability is given by

$$P_{-1} = \frac{V_i}{A} k_{-1} = \frac{\mathrm{MCV} f_w}{A_{cell}} k_{-1} \tag{4}$$

where the additional parameter $f_w = 0.717$ (Raftos et al., 1990) is the fraction of the red cell volume which is accessible to solutes such as glucose. Thus, it is seen that for a system at equilibrium described by equation 2

$$\frac{P_1}{P_{-1}} = \frac{(1 - H_t)k_1}{f_w H_t k_{-1}} = \frac{V_e k_1}{V_i k_{-1}} = 1 \tag{5}$$

Thus, for an equilibrium exchange study such as the magnetization transfer experiment, an identical membrane permeability will be calculated from either the influx or efflux rate constant if the equilibrium condition (eq 2) prevails. However, the permeability and efflux rate constant are independent of the hematocrit (e.g., eq 3), while the influx rate constant does depend on $H_t$.

Although the magnitude of the standard deviations indicates that only in the cases of 6FDG and 4FDG are there significant differences between the α and β anomers, the errors arise primarily from sample-to-sample variations. Since, in each case, α and β rate constants are determined simultaneously on a given sample, the differences are more significant than the standard deviations would suggest. The one exception to this generalization is the case of α-2FDG, for which there is some spectral overlap between intracellular α and extracellular β fluorine resonances. This overlap increases the uncertainty in the determination of $P_\alpha$ for 2FDG. The permeabilities for 3FDG are somewhat lower than the values of 5.8 × $10^{-5}$ and 7.3 × $10^{-5}$ cm/s for 10.2 mM 3FDG reported by Potts and Kuchel (1992); however, the $P_\alpha/P_\beta$ ratio of 1.27 is in excellent agreement with the 1.30 value obtained here (Table 2). This result is also consistent with the independence of the $P_\alpha/P_\beta$ ratio of concentration, which is predicted theoretically (see below) and observed experimentally by Potts and Kuchel (1992).

*Ratio of Permeabilities.* Permeabilities are typically analyzed using phenomenological Michaelis–Menten relations of the form

$$k_1 = \frac{V_{max}}{K_m + [S]} \tag{6}$$

where $K_m$ is the Michaelis constant, $V_{max}$ is the maximal transport velocity, and [S] is the substrate concentration. Equations of this form can be derived using a simple carrier model (Stein, 1986). Thus, the ratio of the permeabilities or rate constants for two species when determined in separate experiments will in general be a function of the $V_{max}$ and $K_m$ values, as well as the substrate concentrations. For the case of two anomers of glucose which are both present in solution simultaneously, the second anomer acts as a competitive inhibitor of the first, giving for the inward rate constant of the β anomer (Stein, 1986; Potts & Kuchel, 1992)

$$k_1^\beta = \frac{V_{max}^\beta}{K^\beta + \frac{K^\beta}{K^\alpha}[\alpha] + [\beta]} = \frac{V_{max}^\beta}{K^\beta\left[1 + \frac{[\alpha]}{K^\alpha} + \frac{[\beta]}{K^\beta}\right]} \tag{7}$$

where $K^\beta$ and $V_{max}^\beta$ are the Michaelis constant and maximal velocities for transport of the β anomer of glucose under equilibrium exchange conditions. As is apparent from the above expression, the α anomer acts as a competitive inhibitor. Similarly, the inward rate constant for the α anomer is given by

$$k_1^\alpha = \frac{V_{max}^\alpha}{K^\alpha + \frac{K^\alpha}{K^\beta}[\beta] + [\alpha]} = \frac{V_{max}^\alpha}{K^\alpha\left[1 + \frac{[\alpha]}{K^\alpha} + \frac{[\beta]}{K^\beta}\right]} \tag{8}$$

where $K^\alpha$ and $V_{max}^\alpha$ are the Michaelis constant and maximum transport velocity for the α anomer under equilibrium exchange conditions. Using these relations, the ratio of the rate constants has the form

$$\frac{k_1^\beta}{k_1^\alpha} = \frac{V_{max}^\beta K^\alpha}{V_{max}^\alpha K^\beta} \tag{9}$$

Thus, the permeability or rate constant ratio is seen to have no explicit dependence on the concentrations if the measurements are made simultaneously on solutions containing both anomers. This relation arises as a consequence of the

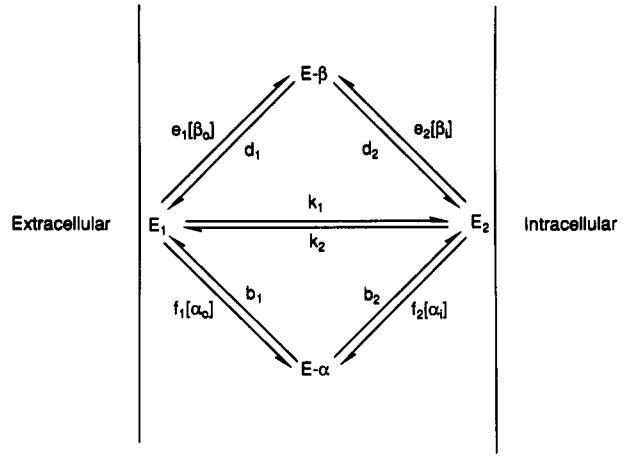


FIGURE 6: Kinetic model used by Stein (1986) to describe the transport of two competing substrates via a simple carrier.

competitive nature of the binding to the transporter by both glucose anomers and would not hold if the anomers were studied singly. The validity of eq 9 is supported by studies of 3FDG transport (Potts & Kuchel, 1992) for which the ratio of transport rates, or equivalently permeabilities, for the two anomers of 3FDG is independent of concentration.

Further analysis of the permeability data requires comparison with various carrier models or the introduction of additional assumptions. Potts and Kuchel (1992) have considered the simple carrier model in the presence of two competing substrates (Figure 6), and although equations of the form of (7) and (8) above were obtained, the parameters $V_{max}^{\alpha}$, $V_{max}^{\beta}$, $K^{\alpha}$, and $K^{\beta}$ given by Potts and Kuchel are functions of concentration. Hence, according to their results, the explicit concentration dependence of the rates is not fully accounted for by eqs 7 and 8. Further, although it is argued that $V_{max}^{\alpha}$ and $V_{max}^{\beta}$ are equal so that eq 9 above reduces to give $k_1^{\beta}/k_1^{\alpha} = K^{\alpha}/K^{\beta}$, this conclusion is not supported in general if $V_{max}^{\alpha}$ and $V_{max}^{\beta}$ are functions of the concentrations. Most significantly, if the Michaelis parameters are functions of concentration, then it is unclear to what extent the observed $k_1^{\beta}/k_1^{\alpha}$ values are biased by the varying concentration ratios of the $\alpha$ and $\beta$ anomers (Table 2). These concerns led us to reevaluate the kinetic analysis using the model of Figure 6. A general solution to the carrier problem outlined in Figure 6 is given by Stein (1986). Stein's eq 23 can be solved in the equilibrium exchange limit appropriate to the present studies by equating intra- and extracellular concentrations of each glucose anomer. After a series of algebraic manipulations, this procedure yields for the relevant Michaelis parameters

$$V_{max}^{\alpha} = \frac{1}{R_{ee}^{\alpha}} = \frac{b_1 b_2}{b_1 + b_2} E_t \tag{10}$$

$$V_{max}^{\beta} = \frac{1}{R_{ee}^{\beta}} = \frac{d_1 d_2}{d_1 + d_2} E_t \tag{11}$$

$$K^{\alpha} = \left(\frac{k_1 + k_2}{k_1 k_2}\right)\left(\frac{b_1 b_2}{b_1 + b_2}\right)\left(\frac{k_1 f_2 + k_2 f_1}{f_1 f_2}\right) \tag{12}$$

$$K^{\beta} = \left(\frac{k_1 + k_2}{k_1 k_2}\right)\left(\frac{d_1 d_2}{d_1 + d_2}\right)\left(\frac{k_1 e_2 + k_2 e_1}{e_1 e_2}\right) \tag{13}$$

where $E_t$ is the total carrier concentration, $R_{ee}^{\alpha}$ and $R_{ee}^{\beta}$ are parameters describing the resistance to equilibrium exchange of each form of the sugar (Stein, 1986), and the rate constants are defined in Figure 6. Thus, we find that, in contrast to the results of Potts and Kuchel, eqs 7 and 8 contain all of the concentration-dependent terms of the kinetic model, and the Michaelis parameters are in fact constants. Combining eqs 9–13, we then obtain for the ratio of the permeabilities or rate constants for the two anomers

$$\frac{k_1^{\beta}}{k_1^{\alpha}} = \left(\frac{k_1 f_2 + k_2 f_1}{f_1 f_2}\right)\left(\frac{e_1 e_2}{k_1 e_2 + k_2 e_1}\right) \tag{14}$$

Thus, the kinetic model of Figure 6 predicts that the ratio $k_1^{\beta}/k_1^{\alpha}$ depends on six rate constants of the model while the expressions for $V_{max}$ depend on the four remaining rate constants. Therefore, within the context of this model, the measured permeability ratio provides no direct information on the parameters which appear in the expressions for $V_{max}$. The assumption of equal $V_{max}$ values for the two anomers (Potts & Kuchel, 1992) is only useful insofar as it allows the complete variation in the observed rates to be assigned to differences between $K^{\alpha}$ and $K^{\beta}$.

Equation 14 above can be further simplified by noting that it depends on only four independent ratios: $R_1 = e_1/f_1$, the ratio of association constants for $\beta$ and $\alpha$ glucose anomers with the carrier on side 1 of the membrane; $R_2 = e_2/f_2$, the corresponding ratio on side 2 of the membrane; $R_3 = e_1/e_2$, the ratio of the association constant for the $\beta$ anomer with the carrier on side 1 relative to that on side 2; and finally $R_4 = k_1/k_2$, reflecting the distribution of the unloaded carrier between the two sides of the membrane. The resulting ratio of glucose influx rate constants is given by

$$\frac{k_1^{\beta}}{k_1^{\alpha}} = \frac{R_1 R_4 + R_2 R_3}{R_3 + R_4} \tag{15}$$

Thus, within the context of the model shown in Figure 6, the measured ratio of rate constants $k_1^{\beta}/k_1^{\alpha}$ depends on only four ratios, of which two, $R_1$ and $R_2$, represent the preference of the carrier for one anomer over the other, the third, $R_3$, represents a difference between the association constants by carrier for one of the anomers depending on which side of the membrane it is on, and the fourth, $R_4$, describes the distribution of the unloaded carrier.

*Spin–Lattice Relaxation.* The above analyses also yield spin–lattice relaxation rates for intra- and extracellular fluorodeoxyglucose pools (Table 2). The ratio of intracellular/extracellular spin–lattice relaxation rates was similar for all of the fluorinated derivatives studied, with a mean value of 2.6. Greater transverse relaxation rates for the intracellular glucose pools are also apparent from the $^{19}F$ spectra. The shorter intracellular relaxation rates presumably indicate reversible binding to intracellular enzyme binding sites, as well as the greater intracellular viscosity (London et al., 1975; Endre et al., 1983).

## DISCUSSION

The replacement of a hydroxyl group by a fluorine substituent results in a structurally homologous molecule but introduces a significant electronic perturbation. Although, as expected, fluorinated carbohydrates are metabolized very differently than their nonfluorinated analogs (Kanazawa et al., 1987; Kojima et al., 1988; Taylor et al., 1988), it might be anticipated that transport behavior would be similar. The primary perturbation of the transport process would presumably arise from alterations in particular hydrogen-bonding interactions with the transporter (Percival & Withers, 1992). Fluorine/hydroxyl substitution has been used previously in order to define critical hydrogen-bonding interactions between

glucose and the transporter (Barnett et al., 1973; Riley & Taylor, 1973). Fluorodeoxyglucose analogs provide an ideal NMR probe of the transport process as a consequence of the resolution of intra- and extracellular pools, the ability to simultaneously observe both glucose anomers, and the retardation of the metabolic transformations of the fluorinated analogs, which allows long-term magnetization transfer studies to be carried out. The NMR method is in turn particularly well-suited for the measurement of rapid transport processes, which are more difficult to study using conventional mix and separate techniques.

The $^{19}F$ resonances of intracellular metabolites are subject to a general downfield shift (London & Gabel, 1989), which may arise due to differences in the extent of hydrogen-bonding interactions between intra- and extracellular compounds. This may reflect differences in the intracellular hydrogen-bonding properties of the water itself, as suggested by Kuchel and co-workers (Kirk & Kuchel, 1988; Xu et al., 1993). Alternatively, intracellular compounds will spend some fraction of time in the vicinity of proteins or other macromolecular structures, so that water is effectively eliminated from the local environment near the fluorine. Hence, at any given time a larger fraction of the intracellular metabolite pools will not be involved in hydrogen-bonding interactions. In addition to hydrogen-bonding interactions, differences in van der Waals contributions to the shielding between intra- and extracellular environment may also be a significant factor in causing the observed shift differences (Gregory & Gerig, 1991). Additionally, intracellular FDG molecules will undergo chemical exchange between the solution and various macromolecular binding sites, including those of the carrier. This exchange is rapid relative to glucose transport (Wang et al., 1986). If these exchange processes are sufficiently rapid on the $^{19}F$ chemical shift scale, the observed shifts will be averaged according to

$$\delta_{obs} = p_F\delta_F + \sum p_i\delta_i \qquad (16)$$

where $\delta_F$ is the shift of the intracellular, uncomplexed FDG, $\delta_i$ are the shifts of the various bound or protein-associated FDG molecules, and $p_i$ are the fractional probabilities. Equation 16 would indicate the existence of a saturable system, with the shifts showing a significant concentration dependence. Studies at 0.2 mM FDG concentrations gave slightly greater intracellular shift values, with all of the values changing fairly uniformly. Hence, this result suggests that any potential binding sites leading to the observed shifts have dissociation constants $\gg$ 10 mM. Alternatively, the use of higher osmotic strength media will lead to a reduction in the intracellular volume and to relative increases in $\sum p_i$ relative to $p_F$, thus increasing the magnitude of the intracellular shift. Shifts of 3FDG were found to depend strongly on extracellular [NaCl], consistent with previous observations for intracellular $^{31}P$ and $^{19}F$ shifts (Xu et al., 1991, 1993). Interestingly, the dependence of $\Delta\beta - \Delta\alpha$ on the position of fluorine substitution did not change greatly with FDG concentration. We note that values for $\Delta\beta - \Delta\alpha$ of 2FDG are subject to a larger error due to overlap of the $\alpha_i$ and $\beta_e$ resonances. Such differences may arise from varying strengths of the hydrogen bonds formed with the fluorines at different positions in the molecule.

Measurements of the anomeric dependence of glucose permeability via the human erythrocyte glucose transporter have historically given mixed results (LeFevre & Marshall, 1958; Faust, 1960; Carruthers & Melchior, 1985; Fujii et al., 1986; Miwa et al., 1988; Potts et al., 1990; Potts & Kuchel, 1992). This variation reflects a number of factors including differences in the experimental conditions, variation in the parameters determined, i.e., whether influx, efflux, or equilibrium exchange is studied, as well as the difficulties inherent in a comparison of relatively small differences measured for species which can interconvert rapidly. The standard deviations in many of these studies are sufficiently large to mask small differences between the anomeric forms (Lowe & Walmsley, 1989). Alternatively, the NMR method is particularly well-suited to such measurements since intracellular and extracellular pools of both anomers can be followed simultaneously, and small differences in anomeric permeability are readily observed. Despite this variability, the present results are consistent with most of the more recent studies in this area. In particular, the more recent $^{19}F$ NMR study of the equilibrium exchange of 3FDG by Potts and Kuchel (1992) as well as the earlier $^{13}C$ NMR study of glucose efflux rates (Kuchel et al., 1987) have also found higher permeability of the $\alpha$ anomer. Stopped-flow measurements of the interconversion of the inward- and outward-facing conformers of the purified glucose transporter in reconstituted red cell membranes have shown that the $\alpha$ anomer of glucose is 37% more effective than the $\beta$ anomer in facilitating interconversion (Appleman & Lienhard, 1989).

The present study also shows that the anomeric dependence of the permeability is not a unique consequence of the 3-fluoro substitution, since the 2-, 3-, 4-, and 6-fluoro derivatives all show a rate preference for the $\alpha$ anomer. This preference also exhibits a significant dependence on the position of the fluorine substitution site, being larger for the 4- and 6-fluoro derivatives. The variation of $P_\beta/P_\alpha$ is also correlated with several other factors. First, the concentration ratio $[\alpha]/[\beta] = f_\alpha/f_\beta$ is smaller for the 4-fluoro and 6-fluoro derivatives than for the 2- and 3-fluoro derivatives (Table 2). However, as shown by the kinetic analysis presented here, the measured permeability ratio is in principle independent of the fractional concentrations of the anomers present. Also, from a quantitative standpoint, the $f_\alpha/f_\beta$ ratio varies by only a factor of 0.67–0.9, significantly smaller than the variation in $P_\beta/P_\alpha$. Second, the $P_\beta/P_\alpha$ ratio also exhibits a rough correlation with the permeability of either anomer. Thus, the 2- and 3-fluoro derivatives, which exhibit the highest permeabilities, show the highest $P_\beta/P_\alpha$ ratio, while the 4- and 6-fluoro derivatives correspond to lower permeabilities and lower $P_\beta/P_\alpha$ ratios.

Within the context of the kinetic model shown in Figure 6, the observed permeability ratio reflects differences in the association rate constants of the carrier for the two anomeric forms. If $R_1 = e_1/f_1 = R_2 = e_2/f_2 = 1$, i.e., neither conformation of the carrier shows an anomeric preference, then no anomeric dependence of $k_1^\beta/k_1^\alpha$, or equivalently $P_\beta/P_\alpha$, is predicted, even if $e_1$ and $e_2$ and/or $f_1$ and $f_2$ and/or $k_1$ and $k_2$ are very different. Thus, the association rate constants on at least one side of the membrane must show some anomeric dependence to observe a permeability ratio different than 1. Additionally, the functional form of eq 14 or 15 predicts that the observed permeability ratio is dominated by the slower kinetic steps. If the anomeric preferences of the carrier for the glucose anomers on the two sides of the membrane differ, i.e., $R_1 \neq R_2$, then the side with the lower association rate constants dominates the observed $k_1^\beta/k_1^\alpha$ ratio. Thus, if $R_3 = e_1/e_2 \ll 1$, the observed ratio will approach the $R_1$ value, which is characteristic of the carrier on side 1 of the membrane. If $R_3 \gg 1$, the observed permeability ratio will approach the limit $R_2$, characteristic of the carrier on side 2 of the membrane. Varying the ratio $R_4$ from 1 displaces the curve but does not alter the limiting values.

Attempts at a more specific analysis lead to two significantly different interpretations. The first possibility is based on the

assumption that the perturbation introduced by the OH/F substitution is global rather than local. Thus, making such a substitution at any position may alter the way in which the anomeric hydroxyl group interacts with the carrier. In this case, any of the association rate constants (except $k_1$ and $k_2$) might be altered by the OH/F substitution. The results could indicate, for example, that making such a substitution at the 4- or 6- position more significantly lowers the $e_1$ or $e_2$ association rate constants of the carrier with the corresponding $\beta$ anomer.

Alternatively, if the OH/F perturbation is viewed as more local, then the primary effect might be to alter the parameter $R_3 = e_1/e_2$, reflecting the relative rate of association with side 1/side 2 of the membrane, rather than parameters $R_1$ or $R_2$, which reflect the relative preference of the carrier for the $\alpha$ and $\beta$ anomers. For example, making the OH/F substitution at a particular position might be expected to reduce both $e_1$ and $f_1$ but to leave the ratio $e_1/f_1$ relatively unchanged. For this case, eq 15 can be viewed as defining a curve for $k_1^\beta/k_1^\alpha$ as a function of $R_3$ which varies from a limit of $k_1^\beta/k_1^\alpha \rightarrow R_1$ for $R_3 \ll 1$ to a limit of $k_1^\beta/k_1^\alpha \rightarrow R_2$ for $R_3 \gg 1$, as discussed above. That is, if the substitution slows down the binding on side 1 of the membrane to a greater extent than the binding to the carrier on side 2, the observed $k_1^\beta/k_1^\alpha$ ratio will be pulled toward $R_1$. The anomeric preferences of the carrier in this conformation will dominate the observed permeability ratio to a greater extent.

Based on the simplest model of the alternating carrier proposed by Barnett et al. (1975), the above kinetic model would reflect reduced association rate constants of the 4-fluoro and 6-fluoro analogs for the carrier when it is on the inner face of the membrane. This conclusion implies that the inward-facing conformation of the carrier exhibits a significant preference for the $\alpha$ anomeric form of the sugars and that binding of the fluorinated sugars to the inward-facing form of the carrier is characterized by lower rate constants than binding to the outward-facing carrier. In this case, the association rate constants with the inward-facing carrier dominate the observed ratio. In fact, the binding event described by the model of Figure 6 is probably a significant oversimplification. The anomeric preference may, for example, reflect the greater difficulty encountered by the inward-facing carrier enclosing the glucose in its $\beta$ configuration.

## REFERENCES


Alger, J. R., & Prestegard, J. H. (1979) *Biophys. J. 28*, 1–14.

Appleman, J. R., & Lienhard, G. E. (1989) *Biochemistry 28*, 8221–8227.

Barnett, J. E. G., Holman, G. D., & Munday, K. A. (1973) *Biochem. J. 131*, 211–221.

Barnett, J. E. G., Holman, G. D., Chalkley, R. A., & Munday, K. A. (1975) *Biochem. J. 145*, 417–429.

Berkowitz, B. A., Moriyama, T., Fales, H. M., Byrd, R. A., & Balaban, R. S. (1990) *J. Biol. Chem. 265*, 12417–12423.

Carruthers, A., & Melchior, D. L. (1985) *Biochemistry 24*, 4244–4250.

Chapman, B. E., & Kuchel, P. W. (1990) *Eur. J. Biophys. 19*, 41–45.

Endre, Z. H., Chapman, B. E., & Kuchel, P. W. (1983) *Biochem. J. 216*, 655–660.

Faust, R. G. (1960) *J. Cell Comp. Physiol. 56*, 103–121.

Fujii, H., Miwa, I., Okuda, J., Tamura, A., & Fujii, T. (1986) *Biochim. Biophys. Acta 883*, 77–82.

Gorga, F. R., & Lienhard, G. E. (1981) *Biochemistry 20*, 5108–5113.

Gregory, D. H., & Gerig, J. T. (1991) *Biopolymers 31*, 845–858.

Kanazawa, Y., Momozono, Y., Yamane, H., Haradahira, T., Maeda, M., & Kojima, M. (1987) *Chem. Pharm. Bull. 35*, 895–897.

Karino, K., Kador, P. F., Berkowitz, B., & Balaban, R. S. (1991) *J. Biol. Chem. 266*, 20970–20975.

Kirk, K., & Kuchel, P. W. (1985) *J. Magn. Reson. 62*, 568–572.

Kirk, K., & Kuchel, P. W. (1988) *Biochemistry 27*, 8803–8810.

Kojima, M., Kuribayashi, S., Kanazawa, Y., Haradahira, T., Maehara, Y., & Endo, H. (1988) *Chem. Pharm. Bull. 36*, 1194–1197.

Krupka, R. M., & Deves, R. (1980) *Biochim. Biophys. Acta 598*, 127–133.

Kuchel, P. W., Chapman, B. E., & Potts, J. R. (1987) *FEBS Lett. 219*, 5–10.

LeFevre, P. G., & Marshall, J. K. (1958) *Am. J. Physiol. 194*, 333–337.

London, R. E., & Gabel, S. A. (1989) *Biochemistry 28*, 2378–2382.

London, R. E., Gregg, C. A., & Matwiyoff, N. A. (1975) *Science 188*, 266–268.

Lopes, D. P., & Taylor, N. F. (1979) *Carbohydr. Res. 73*, 125–134.

Lowe, A. G., & Walmsley, A. R. (1989) in *Red Blood Cell Membranes: Structure, Function, Clinical Implications* (Agre, P., & Parker, J. C., Eds.) pp 597–633, Marcel Dekker, New York.

Macura, S., & Ernst, R. R. (1980) *Mol. Phys. 41*, 95–117.

Miwa, I., Fujii, H., & Okuda, J. (1988) *Biochem. Int. 16*, 111–117.

Nakada, T., & Kwee, I. L. (1986) *Biochem. Arch. 2*, 53–61.

Nakada, T., Kwee, I. L., & Conboy, C. B. (1986) *J. Neurochem. 46*, 198–201.

Percival, M. D., & Withers, S. G. (1992) *Biochemistry 31*, 498–505.

Perrin, C. L., & Engler, R. E. (1990) *J. Magn. Reson. 90*, 363–369.

Potts, J. R., & Kuchel, P. W. (1992) *Biochem. J. 281*, 753–759.

Potts, J. R., Hounslow, A. M., & Kuchel, P. W. (1990) *Biochem. J. 266*, 925–928.

Raftos, J. E., Bulliman, B. E., & Kuchel, P. W. (1990) *J. Gen. Physiol. 95*, 1183–1204.

Riley, G. J., & Taylor, N. F. (1973) *Biochem. J. 135*, 773–777.

Robinson, G., Kuchel, P. W., Chapman, B. E., Doddrell, D. M., & Irving, M. G. (1985) *J. Magn. Reson. 63*, 314–319.

Sachs, W. (1968) *Arch. Biochem. Biophys. 123*, 507–513.

Stein, W. D. (1986) *Transport and Diffusion Across Cell Membranes*, Chapter 4, Academic Press, New York.

Taylor, N. F., Sbrissa, D., Squire, S. T., D'Amore, T., & McIntosh, J. M. (1988) in *Fluorinated Carbohydrates, Chemical and Biochemical Aspects* (Taylor, N. F., Ed.) ACS Symposium Series 374, pp 109–137, American Chemical Society, Washington, DC.

Tewson, T. J., Welch, M. J., & Raichle, M. E. (1978) *J. Nucl. Med. 19*, 1339–1345.

Vyska, K., Mehdorn, H. M., Machulla, H.-J., & Knust, E. J. (1985) *Neurol. Res. 7*, 63–67.

Walmsley, A. R. (1988) *Trends Biochem. Sci. 13*, 226–231.

Wang, J.-F., Falke, J. J., & Chan, S. I. (1986) *Proc. Natl. Acad. Sci. U.S.A. 83*, 3277–3281.

Wheeler, T. J., & Hinkle, P. C. (1985) *Annu. Rev. Physiol. 47*, 503–517.

Xu, A. S. L., Potts, J. R., & Kuchel, P. W. (1991) *Magn. Reson. Med. 18*, 193–198.

Xu, A. S. L., Waldeck, A. R., & Kuchel, P. W. (1993) *NMR Biomed. 6*, 136–143.